Applied Catalysis B: Environmental 128 (2012) 159–170

Contents lists available at SciVerse ScienceDirect

Applied Catalysis B: Environmental

journal homepage: www.elsevier.com/locate/apcatb

# Key parameters influencing the performance of photocatalytic oxidation (PCO) air purification under realistic indoor conditions

Hugo Destaillats[a,b,*], Mohamad Sleiman[a], Douglas P. Sullivan[a], Catherine Jacquiod[c], Jean Sablayrolles[d], Laurent Molins[c]

[a] Lawrence Berkeley National Laboratory, Indoor Environment Group, 1 Cyclotron Road MS 70-108B, Berkeley, 94720 CA, USA
[b] Arizona State University, Department of Chemistry & Biochemistry, Tempe, 85287 AZ, USA
[c] Saint Gobain Quartz, 108 Av. Carnot, 77140 Saint Pierre les Nemours, France
[d] Saint Gobain Recherche, 39 quai Lucien Lefranc, 93300, Aubervilliers, France

ARTICLE INFO

*Article history:*
Available online 14 April 2012

*Keywords:*
Photocatalysis
Air cleaner
Indoor air quality
Aldehydes
HVAC

ABSTRACT

Photocatalytic oxidation (PCO) air cleaning is a promising technology suitable for the elimination of a broad range of volatile organic compounds (VOCs). However, performance of poorly designed PCO systems may be affected by the formation of volatile aldehydes and other partially oxidized byproducts. This study explored the role of key design and dimensioning parameters that influence the effective removal of primary pollutants and can help reduce or eliminate the formation of secondary byproducts. A model pollutant mixture containing benzene, toluene, o-xylene, undecane, 1-butanol, formaldehyde and acetaldehyde was introduced at a constant rate in a 20-$m^3$ environmental chamber operating at an air exchange rate of 1 $h^{-1}$. Individual pollutant concentrations were kept at realistically low levels, between 2 and 40 $\mu g\,m^{-3}$. A prototype air cleaner provided with flat or pleated PCO filtering media was operated in an external ductwork loop that recirculated chamber air at flow rates in the range 178–878 $m^3\,h^{-1}$, corresponding to recycle ratios between 8.5 and 38. Air samples were collected upstream and downstream of the air cleaner and analyzed off-line to determine single-pass removal efficiency. The final-to-initial chamber concentration ratio was used to determine the global chamber removal efficiency for each pollutant. In the flat filter configuration, longer dwelling times of compounds on the $TiO_2$ surface were attained by reducing the recirculation airflow by a factor of ~5, leading to increasing total pollutant removal efficiency from 5% to 44%. Net acetaldehyde and formaldehyde removal was achieved, the later at airflow rates below 300 $m^3\,h^{-1}$, illustrating the critical importance of controlling the contact time of primary and secondary pollutants with the $TiO_2$ surface. The use of pleated media was shown to increase significantly the system performance by extending the dwelling time of pollutants on the irradiated surface of the PCO media, with a 70% degradation of target pollutants. With the pleated media, formaldehyde removal efficiency increased to 60%. Irradiation using either a UVC or a UVA lamp under identical flow conditions produced similar pollutant elimination. A simple correlation between the steady-state single pass removal efficiency and the global chamber removal efficiency was used to rationalize these experimental results and identify optimal operating conditions.

Published by Elsevier B.V.

## 1. Introduction

An estimated 10% of the total energy consumed by the U.S. commercial building stock is used to condition ventilation air [1,2]. Hence, significant energy savings can be achieved in the built environment, among other approaches, by tightening the building envelope and reducing ventilation rates. These strategies require parallel implementation of countermeasures to preserve acceptable indoor air quality, including source controls and the operation of advanced air cleaning technologies. For example, achieving 50% reduction in outdoor air ventilation in a typical US building would require a pollutant removal efficiency of 15–20% in order to prevent increased occupant exposures to volatile organic compounds (VOCs) [3,4].

Photocatalytic oxidation (PCO) is a promising technology for indoor air purification [5–7]. It can decompose a broad spectrum of VOCs containing multiple chemical functionalities, including several that are poorly removed by other methods. For example, formaldehyde is not efficiently removed by air

* Corresponding author at: Lawrence Berkeley National Laboratory, Environmental Energy Technologies Division, 1 Cyclotron Road, MS 70-108B, Berkeley, CA 94720, United States. Tel.: +1 510 486 5897; fax: +1 510 486 7303.
*E-mail addresses:* HDestaillats@lbl.gov (H. Destaillats), Laurent.LM.Molins@saint-gobain.com (L. Molins).

0926-3373/$ – see front matter. Published by Elsevier B.V.
doi:10.1016/j.apcatb.2012.03.014

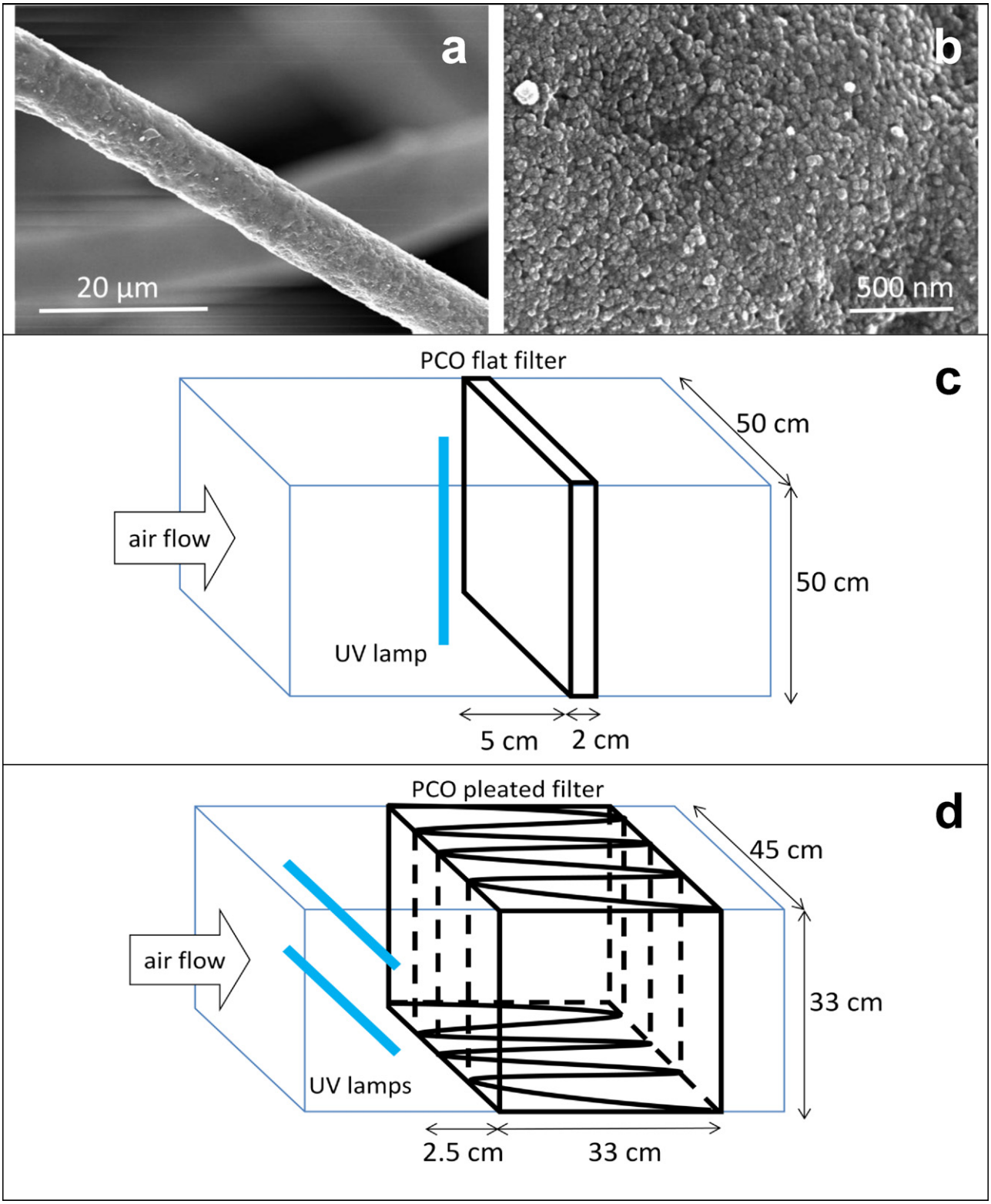


**Fig. 1.** (a) SEM image of PCO media fiber; (b) SEM image of $TiO_2$ fiber coating; (c) flat filter configuration; (d) pleated filter configuration.

cleaning methods based on adsorption (e.g., activated carbon containing media) [3]. Other advantages include relatively low cost and maintenance of PCO systems and the use of non-toxic catalysts. Multiple factors have been observed to affect the efficiency of PCO air cleaners for indoor air applications [8]. Significant research efforts have been devoted to the optimization of photocatalytic reactor design [9–14] and supported $TiO_2$-based catalysts [15–19]. However, the formation of partially oxidized byproducts, and specifically volatile aldehydes such as formaldehyde and acetaldehyde, is a concern that remains to be fully addressed. Such byproducts are generated in the photocatalytic oxidation of various VOCs, as shown in experiments performed

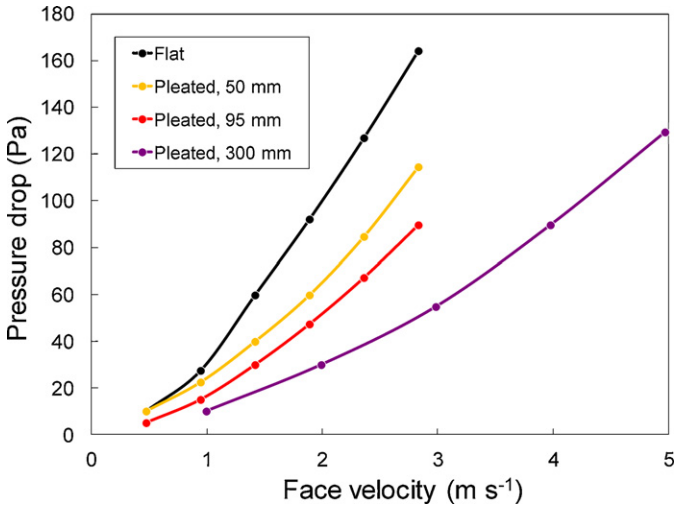


**Fig. 2.** Dependence of the pressure drop on the face velocity for flat and pleated PCO media with a $TiO_2$ loading of 80 g $m^2$.

with full-scale chamber settings [20–22] and bench-scale experiments [23].

Advancement of PCO air cleaning technologies requires identifying the optimal tests that will challenge the system under realistic conditions that include low (part-per-billion) pollutant concentrations, the presence of a VOC mixture representative of typical indoor contaminants and the use of flow conditions that are consistent with those encountered in buildings, e.g. face velocities typical of heating, ventilation and air conditioning (HVAC) systems. There is an international consensus on the need for reliable standardization of testing methods for air cleaning technologies.

The goal of this study was to evaluate the performance of a PCO air cleaner prototype under realistic conditions. We have carried out experiments to evaluate the effectiveness of the PCO unit in reducing chamber concentrations of target pollutants while minimizing or avoiding the formation of secondary byproducts. Key system parameters were investigated, including the effect of the recirculating airflow rate (or the recycle ratio), the effect of the type of irradiation and the geometry of the PCO media.

## 2. Experimental methods

### 2.1. PCO media

We used two different types of PCO filters, flat and pleated, fabricated with QUARTZEL® photocatalytic media. The media consisted of $TiO_2$-coated quartz fibers of 9 μm diameter pressed into a 20-mm thick felt. $TiO_2$ particles were deposited on quartz fibers through a sol–gel process, and had a BET specific surface area of 120 $m^2$ $g^{-1}$.The areal weight of the uncoated felt was 80 g $m^{-2}$; it increased to 120 g $m^{-2}$ after the media was coated with titania. Due to the different geometries corresponding to the flat and pleated media configuration, the mass of $TiO_2$ in the system was 10 g and 32 g, respectively. The corresponding specific surfaces were 1200 $m^2$ and 3840 $m^2$. Irradiation of the media was performed with 36-W UVC and UVA fluorescent tubes (Phillips PL-L series). Fig. 1 illustrates scanning electron microscopy (SEM) images of the coated fibers, as well as the configuration and dimensions of the PCO filters used in this study.

Fig. 2 describes the dependence of the pressure drop across the PCO media as a function of the face velocity, for a flat filter as well as for three different pleated filters of depth 50, 95 and 300 mm. The latter corresponds to the pleated filter used in our experiment. Pressure drop was measured in a separate test, following the ANSI/ASHRAE 52.2-2007 standard [24].

### 2.2. Room-sized environmental chamber setup

The chamber setup used in this study is described in Fig. 3. Target VOCs and volatile carbonyls were introduced at a constant rate into a 20-$m^3$ environmental chamber that was ventilated at a constant air exchange rate of 1 $h^{-1}$. The chamber was built entirely of stainless-steel to minimize surface losses of analytes, allowing for accurate determinations at low part-per-billion levels. The PCO unit was installed on an external ductwork loop and operated in recirculation mode, by re-introducing the air processed by the PCO air cleaner into the chamber. Outdoor air was pre-cleaned with a HEPA filter and a bed containing activated carbon and $KMnO_4$-coated chemisorbent media (Purafil SP) that removed organic traces before being introduced into the chamber by a variable-speed fan. An independent variable-speed fan operating inside the chamber was used to recirculate chamber air through an external ductwork loop in which the PCO unit was placed. Sampling ports were installed on the loop upstream and downstream from the PCO unit.

A liquid VOC mixture, consisting of o-xylene, undecane, benzene, 1-butanol and toluene, was prepared in the proportions required to generate the target gas phase concentrations. The composition of the VOC mixture was adjusted in preliminary tests. The mixture was placed in a glass syringe and introduced at a constant rate into chamber air by means of a mechanical syringe pump at a flow rate between 1 and 12 μL $h^{-1}$.

Commercial formaldehyde aqueous solutions are commonly stabilized with methanol and should not be used to generate gas phase formaldehyde mixtures to prevent the presence of the alcohol in chamber air. For that reason, we prepared periodically stock aqueous solutions of formaldehyde by dissolving paraformaldehyde in boiling water under reflux. An aqueous mixture containing formaldehyde and acetaldehyde was prepared in the approximate

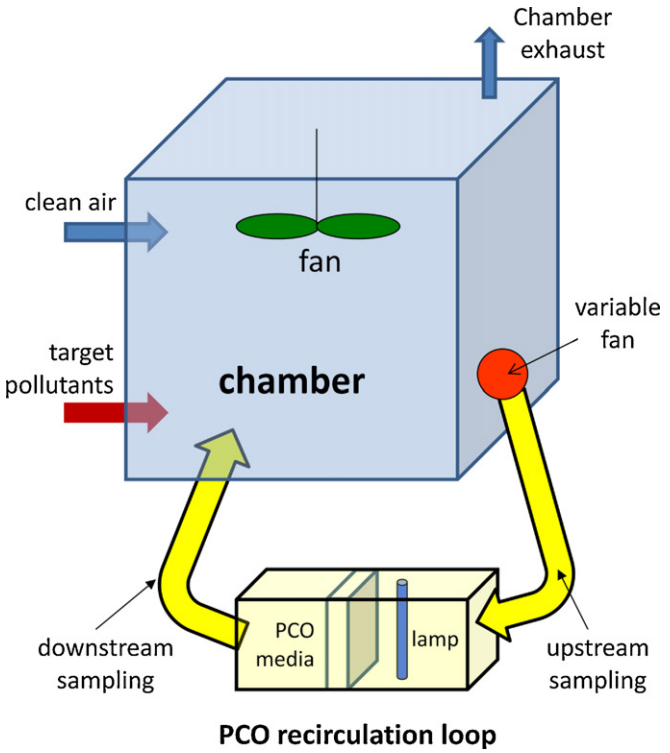


**Fig. 3.** Schematic of 20-$m^3$ stainless-steel chamber with external PCO recirculation loop.

proportions required to generate the corresponding target gas phase concentrations in the chamber. The mixture was placed in a separate glass syringe and introduced at a constant rate (between 100 and 300 $\mu L\,h^{-1}$) into chamber air by means of a second syringe pump. The end of the needle was heated to evaporate the solution upon introduction into the chamber.

### 2.3. Sampling and analytical methods

Samples of VOC and volatile carbonyls were collected simultaneously upstream and downstream of the PCO unit at different times. Upstream samples corresponded to chamber concentrations, and downstream samples corresponded to pollutant levels exiting the PCO unit before being mixed with chamber air.

VOC samples were collected in Tenax-TA® sorbent tubes (Supelco) over periods of 30–90 min. The concentration value reported in each case corresponds to a time-integrated average over the sampled period, and is reported at the center of each sampling period. Air was drawn through the sorbent tubes by means of peristaltic pumps operating in the range 30–100 $cm^3\,min^{-1}$. The flow corresponding to each sample was measured using a primary air flow calibrator (Gilibrator®) with a precision better than 1%. Volatile carbonyl samples were collected in dinitrophenyl hydrazine (DNPH)-coated silica samplers (Waters) over periods of identical duration as those of the VOC samples. The concentration value reported in each case corresponds to a time-integrated average over the sampled period, and is reported at the center of each sampling period. Air was drawn through the aldehyde samplers by means of peristaltic pumps operating at ~1 $L\,min^{-1}$. The flow corresponding to each sample was measured using a primary air flow calibrator (Gilibrator®) with a precision better than 2%.

Tenax sorbent tubes were analyzed by thermal desorption/gas chromatography/mass spectrometry (TD/GC/MS, Gerstel/Agilent) operated in electron impact mode, following the standard TO-1 EPA method [25]. A DB-5 chromatographic column (Agilent J&W) was used with TD desorption at 250 °C and trapping at −10 °C. The GC temperature program consisted on a 5 °C $min^{-1}$ ramp between 1 °C and 220 °C. Bromofluorobenzene was added to each tube and used as internal standard for quantification. Calibration curves for each analyte were performed in the range 5–150 ng, using characteristic MS ions of each analyte by injecting known amounts of authentic standards in precleaned Tenax tubes. The detection limit for each VOC was typically 1 ng or lower, corresponding to chamber concentrations <0.1 $\mu g\,m^{-3}$. DNPH cartridges were extracted with 2-mL aliquots acetonitrile, and the extracts were analyzed by HPLC with UV detection at 360 nm following a US EPA method [26]. A calibration curve for quantification was carried out using authentic standards of the DNPH hydrazone of formaldehyde, acetaldehyde and acetone. A calibration curve for propanal and butanal was carried out by injecting a known amount of each of those compounds in a clean DNPH sampler, and extracting in acetonitrile following the procedure described above. The detection limit for each volatile carbonyl determined by the DNPH/HPLC method was typically 10 ng or lower, corresponding to chamber concentrations <0.1 $\mu g\,m^{-3}$.

### 2.4. Determination of chamber operation conditions

The operation conditions are summarized in Table 1. In all experiments, the chamber was kept at a constant ventilation rate between 21 and 23 $m^3\,h^{-1}$, corresponding to an air exchange rate of $\lambda \approx 1\,h^{-1}$. The chamber airflow was recorded continuously with a turbine flow meter, the reported value being the average over the duration of the experiment ± one standard deviation. The air exchange rate was verified independently between experiments by injecting a pulse of $CO_2$ (inert tracer) and following its decay with a $CO_2$ monitor. The chamber was maintained at a slight overpressure with respect to the laboratory, measured and logged with an APT detector (Energy Conservatory, MN). Temperature and relative humidity (RH) were kept close to ambient levels, and logged continuously with the same device. These parameters are also reported as a time average over the duration of the experiment ± one standard deviation. Previous studies using a similar type of PCO media have shown that RH variations had an effect on the kinetics of the photocatalyzed reactions, the extent of pollutant adsorption and removal [27]. For that reason, we kept RH constant in the range 20–30% to compare all experiments under the same conditions.

The PCO loop recirculation rate was varied between 150 and 900 $m^3\,h^{-1}$, corresponding to recycle ratios in the range $8 < \rho < 40$ (defined as the ratio between the airflow in the recirculation loop and the chamber ventilation airflow). The loop recirculation rate was adjusted using a combination of a variable fan and iris aperture. The airflow at the loop was measured with a calibrated Venturi tube by measuring the pressure differential at both sides of the iris damper. The pressure drop across the PCO media was measured and recorded with the APT detector. The face velocity was determined directly as the ratio between the loop airflow and the perpendicular aperture of the PCO filter. Similarly, the residence time (space time) of a parcel of air inside the PCO media was determined as the ratio between the volume of media exposed and the air flowrate in the loop.

**Table 1**
Summary of experimental conditions used in each test.

| Experiment # | 1 | 2 | 3 | 4 | 5 | 6 |
|---|---|---|---|---|---|---|
| | No PCO filter | Flat PCO filter | | | | Pleated PCO filter |
| Chamber conditions | | | | | | |
| Air circulation rate ($m^3\,h^{-1}$) | 23.6 ± 0.6 | 23.4 ± 0.5 | 22.9 ± 0.6 | 20.9 ± 0.2 | 20.9 ± 0.1 | 20.7 ± 0.1 |
| Air exchange rate, $\lambda$ ($h^{-1}$) | 1.08 | 1.08 | 1.07 | 0.98 | 0.98 | 0.97 |
| Overpressure (Pa) | 1.3 ± 0.1 | 1.3 ± 0.1 | 2.4 ± 0.1 | 0.9 ± 0.3 | 0.5 ± 0.1 | 1.8 ± 0.2 |
| Temperature (°C) | 30 ± 3 | 28 ± 1 | 28 ± 1 | 27 ± 1 | 28 ± 1 | 27 ± 1 |
| Relative humidity (%) | 20 ± 4 | 23 ± 2 | 23 ± 3 | 30 ± 3 | 26 ± 2 | 25 ± 4 |
| PCO loop conditions | | | | | | |
| Recirculation rate ($m^3\,h^{-1}$) | 373 ± 6 | 354 ± 6 | 878 ± 7 | 178 ± 22 | 193 ± 25 | 365 ± 8 |
| Recycle ratio ($\rho$) | 15.8 | 15.1 | 38.3 | 8.5 | 9.2 | 17.6 |
| Pressure drop across PCO media, $\Delta P_{PCO}$ (Pa) | – | 13.8 ± 0.3 | 38.8 ± 0.5 | 5.42 ± 0.32 | 6.40 ± 0.28 | 2.7 ± 0.2 |
| Face velocity ($m\,s^{-1}$) | n.a. | 0.39 | 0.97 | 0.20 | 0.21 | 0.68 |
| PCO residence time (ms) | n.a. | 65 | 27 | 132 | 122 | 159 |
| Irradiation type | No UV | UVC | UVC | UVC | UVA | UVA |
| Max. irradiance ($mW\,cm^{-2}$) | – | 8.0 | 8.0 | 8.0 | 5.9 | 6.1 |

n.a.: does not apply to this experimental condition.

**Table 2**
Chamber background, target levels and reported indoor levels for the model indoor pollutants introduced in the environmental chamber.

| Compound | Chamber background ($\mu g\,m^{-3}$) | Target level ($\mu g\,m^{-3}$) | Indoor levels reported in the literature[a] ($\mu g\,m^{-3}$) | | | |
|---|---|---|---|---|---|---|
| | | | Median | | 90‰ | |
| | | | Residential | Office | Residential | Office |
| Benzene | < 0.1 | 2–3 | 2.8<br>4.7[b]<br>0.8[c] | 3.1 | 10<br>8.3[b]<br>4.3[c] | 11 |
| Toluene | < 0.1 | 10–15 | 12.4<br>9.5[c] | 7.9 | 45<br>42[c] | 28.6 |
| o-Xylene | < 0.1 | 2–3 | 2.2<br>1.1[c] | 2.8 | 7.7<br>4.7[c] | 10.2 |
| n-Undecane[d] | < 0.1 | 6–10 | 1.3<br>0.9[c] | 1.9 | 4.7<br>5.2[c] | 6.8 |
| 1-Butanol[e] | < 0.1 | 2–3 | 1.6[c] | | 3.9[c] | |
| Formaldehyde | 3–5 | 20–35 | 21<br>36[c] | | 75<br>86[c] | |
| Acetaldehyde | 1–3 | 20–45 | 5.5<br>19[c] | | 20<br>55[c] | |
| Acetone | 2–4 | – | | | | |

[a] Hodgson and Levin, 2003 (unless stated otherwise) [33].
[b] Shimmer et al., 2005 [34].
[c] Offerman, 2009 [35].
[d] Literature values are for n-nonane and n-hexane.
[e] Literature values are for phenol.

Irradiance measurements were performed at the face of the PCO media using a calibrated radiometer provided with two probes, one for UVC light at 254 nm and the other for UVA light at 365 nm (UVP Inc., Upland, CA). For the flat filter configuration, irradiance measurements were performed for the UVC and the UVA lamp by placing the probe at nine different positions. Three of the measurements were performed along the lamp's axis at a $50 \pm 2$ mm distance from the lamp, and corresponded to the maximum intensity at an incidence angle of 0°. The other six determinations were made along lines parallel to the lamp's axis, three at each side and equidistant to the center, at $182 \pm 4$ mm with an incidence angle of 70°. In the case of the UVC lamp, irradiance measured at the central positions ranged between 7 and 8 mW cm$^{-2}$, and values determined at the sides were between 0.2 and 0.4 mW cm$^{-2}$. For the UVA lamp, irradiance measured at the central positions was between 4.5 and 6 mW cm$^{-2}$, and values determined at the sides were between 0.15 and 0.3 mW cm$^{-2}$. Irradiance measurements for the pleated filter configuration were performed in a similar manner, by measuring a total of 27 values on three different planes with respect to the position of the lamps (only UVA was used in this case). Nine measurements were made at the front of the filter, nine at the middle and nine at the back (2.5, 19 and 35 cm from the lamp, respectively). Measurements performed at positions that were facing directly one of the two lamps in the front of the filter corresponded to the maximum irradiances, in the 4.6–6 mW cm$^{-2}$ range. Positions in the back of the filter were those with the lowest irradiance, between 0.7 and 1 mW cm$^{-2}$.

### 2.5. Determination of chamber background pollutant levels

Background levels were determined in the chamber before each experiment. Table 2 reports concentrations measured for each compound in a well-ventilated chamber without injection of the target pollutant mixture. We could not detect measurable amounts of most of the studied compounds in the background. However, low levels of formaldehyde, acetaldehyde and acetone were observed. The activated carbon/chemisorbent bed was efficient in removing low level VOCs from inlet air, but was not able to completely reduce the concentration of volatile carbonyls to zero. Our target concentration for formaldehyde and acetaldehyde were well above the background levels. Target concentrations for the seven compounds introduced in the chamber were consistent with values reported in the literature for their indoor concentrations, also summarized in Table 2.

### 2.6. Evaluation of the stability of the pollutant source

In an initial test (Experiment #1), the chamber and the loop were operated at steady state for 100 h in the absence of the PCO filter, to evaluate the stability in the concentration of target pollutants injected at a constant rate over that period. Fig. 4 shows the concentration profiles observed for four of the compounds during the stability test, which are representative of the whole mixture. At $t = 0$ the syringe pumps (pollutant sources) were turned on.

Each experimental data point corresponds to the average of two simultaneous determinations. The individual error bars correspond to the difference between those determinations. Open data points were used for upstream measurements and solid blue data points for downstream measurements with respect to the position of the PCO filter. In each figure, we indicated the average of all samples measured at $t > 20$ h with a red dotted line. The average ± one standard deviation was indicated with green dotted lines above and below the average concentration. The concentrations of admitted compounds reach a steady state at (or before) 10 h of operation, consistent with simple mass-transfer modeling predictions. The concentration fluctuations were significantly greater than the experimental error of each pair of duplicate determinations. The analytical methodology proved sensitive enough to detect fluctuations in the gas phase concentrations of target pollutants during the course of several days of continuous operation. While the uncertainty of most duplicate determinations was 3–5%, the relative standard deviations of mean chamber concentrations taken over the period $10\,h < t < 100\,h$ were significantly larger, in most cases in the order of 15%. We take the latter as a conservative estimation of the experimental error in the determination of chamber concentrations at low part-per-billion levels. Fluctuations

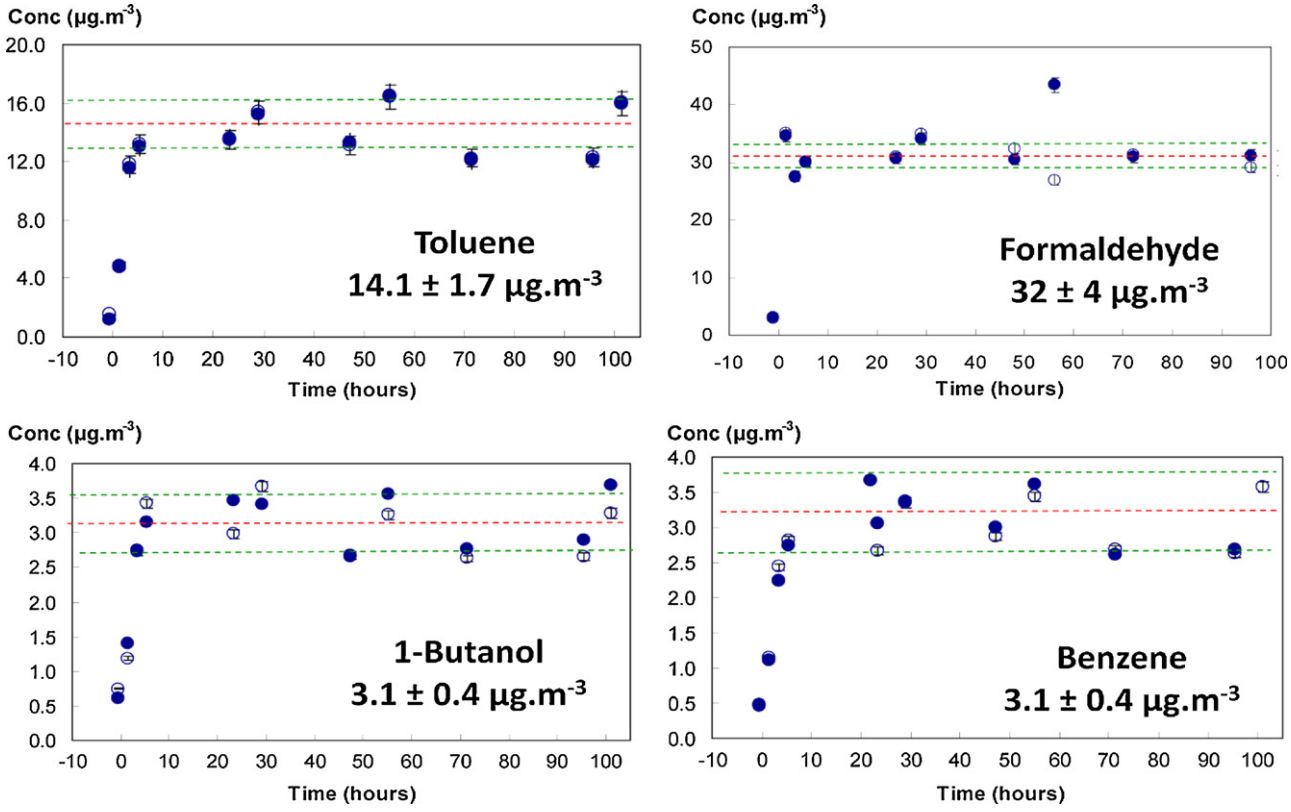


**Fig. 4.** 100-h stability test for selected model pollutants injected at a constant rate in the 20-m$^3$ chamber (Experiment #1). Open circles correspond to upstream concentrations, solid circles correspond to downstream concentrations.

were likely related to variations in chamber temperature during daily cycles and instabilities in the syringe pumps (e.g., presence of bubbles in the injected liquid).

### 2.7. Evaluation of the effect of sorbed species on PCO media

During preliminary tests, we observed effects attributable to sorption and desorption of target compounds to the PCO media. When the PCO media was present during the equilibration period prior to turning on the UV lamp, the high surface area of the photoactive felt served as a sink for gas-phase species. Subsequently, those compounds were driven off the surface of the media by the heat generated by the UV lamp, increasing chamber concentrations. This effect was observed only when the VOC concentrations were very low, as illustrated in Fig. 5: at high initial concentrations (36 µg m$^{-3}$) of o-xylene pre-equilibrated with the PCO media, its concentration was reduced over time under UV irradiation without any visible desorption of the analyte from the filter (Fig. 5a). Instead, when its initial concentration was decreased by one order of magnitude to 4 µg m$^{-3}$, heating of the PCO media by the UV lamp led to a transient increase in o-xylene concentration, that compensated for pollutant degradation during the early stages of the reaction (Fig. 5b). The same effect was observed for all other analytes, and may lead to underestimation of the removal efficiency of PCO air cleaners if the system is not allowed to operate for a long enough period to reach a final steady-state condition.

In order to minimize these experimental artifacts affecting low-ppb measurements, in experiments performed with the flat PCO filter (#2 to #5) we did not pre-equilibrate VOCs with the media. Instead, the filter was introduced at $t = 0$, simultaneously with turning on the UV lamp. Prior to its introduction into the system, the filter was kept in a sealed Teflon bag to minimize contamination of the media surface. Fig. 5c illustrates the curve obtained for o-xylene at low concentration when the media was introduced at $t = 0$. During the initial transient period, photocatalytic elimination of the pollutant took place in parallel with reversible adsorption to the media, leading to lower concentrations that those achieved purely by photocatalytic elimination. Only after 30 h of continuous irradiation the system reached a steady-state condition in which the analyte equilibrated with the irradiated media. For that reason, we determined the removal efficiency by considering only samples at $t > 30$ h to be representative of the final steady-state condition for experiments with the flat PCO filter.

## 3. Results and discussion

The initial and final chamber concentrations determined in each experiment performed with the flat PCO media (Experiments #2 to #5) and the pleated media (Experiments #6) are reported in Table 3. Acetone is included in the table because it is the only compound that was present in chamber background air at significant levels. No other byproduct was observed to be formed by the PCO reaction, except for very small (<0.2 µg m$^{-3}$) amounts of propanal and butanal. Recent studies report the formation of other byproducts in PCO decomposition of aromatic compounds, such as benzaldehyde and cresols [21]. However, due to the low concentrations used in this study, we did not observe those byproducts. The final steady-state concentrations were determined as an average of determinations at $t > 30$ h. While several individual determinations have very good precision, with relative experimental errors as low as 3–5%, in many other cases relative errors were higher (e.g., 20–40%). In average, the experimental errors are between 7 and 10% for experiments performed with the flat filter. In the experiment performed with the pleated filter, the average relative experimental

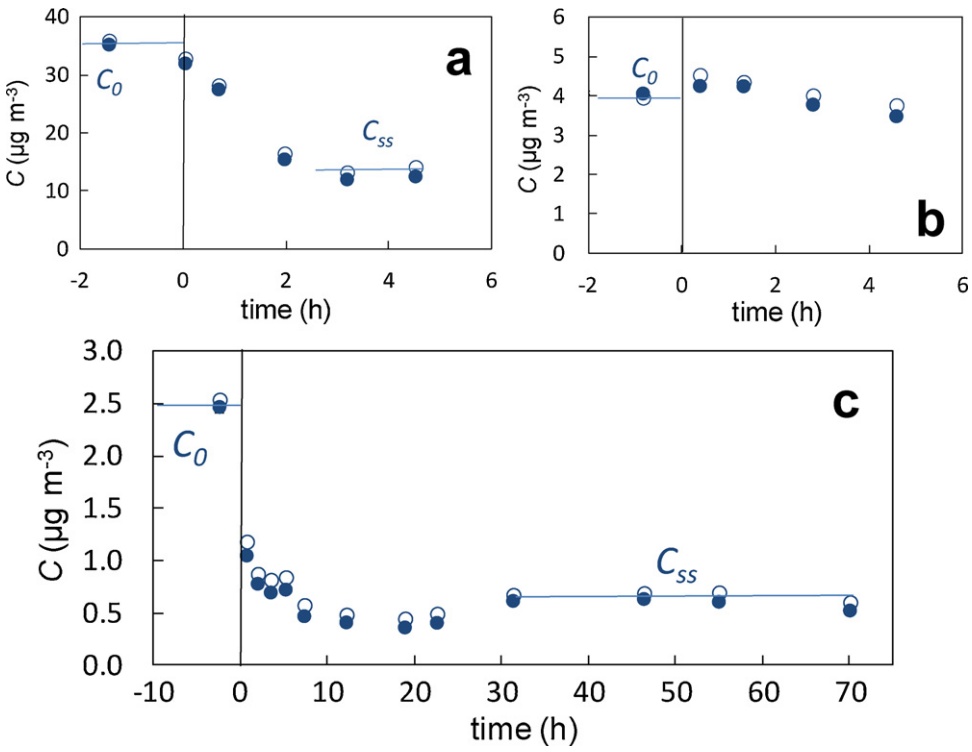


**Fig. 5.** Concentration profiles of o-xylene for (a) pre-equilibration of PCO media in the dark at high VOC concentrations and high recycle ratio ($\rho = 38$); (b) pre-equilibration of PCO media in the dark at low VOC concentrations and $\rho = 15$; (c) introduction of PCO media at $t = 0$ at low VOC concentrations and $\rho = 15$. Open circles correspond to upstream concentrations, solid circles correspond to downstream concentrations.

errors were higher (15%), mostly because the final concentrations were lower than in experiments with the flat filter. These results are consistent with our previous discussion on the stability of the pollutant source (Section 2.6).

### 3.1. Effect of the residence time

Three of the experiments using a flat PCO filter (Experiments #2, 3 and 4) were carried out in identical experimental conditions except for the recirculation rate, which was varied between 178 and 878 $m^3\ h^{-1}$. The results allowed us to observe the effect of the residence time on the removal efficiency ($R$) of target pollutants. Contrary to the intuitive misperception that a higher recycle ratio would lead to improved air cleaning efficiency simply by processing more air per unit time, our results show clearly that the opposite trend is true. This is consistent with results summarized by Zhong et al. [8] and with observations from recent experiments performed in bench-scale reactors [28] and in the pilot scale [29]. The total concentration of compounds in the chamber (calculated by adding all measured VOC and aldehyde levels) decreased marginally (5%) for the experiment performed at the higher recycle ratio of $\rho = 38$, by 18% for $\rho = 15$ and by 44% for the lowest recycle ratio ($\rho = 8.5$).

Increasing the contact time between pollutants and the PCO media by decreasing the recycle ratio is a critical factor that improved PCO performance, as shown in Fig. 6a. The residence time of a parcel of air was calculated using geometrical considerations and the volumetric flow rate, but the dwelling time of a specific compound in the dense PCO media is likely longer than the residence time of air, due to a sequence of multiple adsorption and desorption cycles inside the media. It is also likely that the dwelling time of less volatile compounds in the PCO media is longer than that of more volatile species. We observed that the less volatile species (undecane, o-xylene and 1-butanol) are

**Table 3**
Initial ($C_0$) and final steady-state ($C_{ss}$) chamber concentrations of model pollutants.

| | o-Xylene | Undecane | Benzene | 1-Butanol | Toluene | Formaldehyde | Acetaldehyde | Acetone | Total |
|---|---|---|---|---|---|---|---|---|---|
| Experiment #2 (flat filter, $\rho = 15.1$, UVC) | | | | | | | | | |
| $C_0$ ($\mu g\ m^{-3}$) | 2.5 ± 0.1 | 11.0 ± 0.5 | 2.9 ± 0.1 | 2.8 ± 0.3 | 12.7 ± 0.6 | 30 ± 1 | 42 ± 1 | 5.5 ± 2.0 | 110 ± 5 |
| $C_{ss}$ ($\mu g\ m^{-3}$) | 0.6 ± 0.1 | 2.2 ± 0.5 | 2.5 ± 0.1 | 0.4 ± 0.1 | 7.5 ± 0.2 | 44 ± 1 | 26.8 ± 0.3 | 6.1 ± 0.3 | 90 ± 2 |
| Experiment #3 (flat filter, $\rho = 38$, UVC) | | | | | | | | | |
| $C_0$ ($\mu g\ m^{-3}$) | 2.1 ± 0.1 | 9.4 ± 0.7 | 2.3 ± 0.1 | 2.2 ± 0.1 | 10.6 ± 0.7 | 20 ± 1 | 29 ± 1 | 4.1 ± 0.3 | 80 ± 3 |
| $C_{ss}$ ($\mu g\ m^{-3}$) | 0.9 ± 0.1 | 3.3 ± 0.1 | 2.0 ± 0.1 | 0.6 ± 0.1 | 7.8 ± 0.2 | 33 ± 1 | 21.7 ± 0.3 | 5.9 ± 0.7 | 76 ± 4 |
| Experiment #4 (flat filter, $\rho = 8.5$, UVC) | | | | | | | | | |
| $C_0$ ($\mu g\ m^{-3}$) | 2.9 ± 0.1 | 10.5 ± 0.5 | 3.3 ± 0.1 | 3.4 ± 0.1 | 15.2 ± 0.1 | 29 ± 5 | 47 ± 3 | 2.0 ± 0.1 | 113 ± 8 |
| $C_{ss}$ ($\mu g\ m^{-3}$) | 0.8 ± 0.1 | 2.6 ± 0.1 | 2.3 ± 0.1 | 0.5 ± 0.1 | 7.7 ± 0.4 | 22 ± 3 | 23 ± 1 | 4.6 ± 0.2 | 63 ± 4 |
| Experiment #5 (flat filter, $\rho = 9.2$, UVA) | | | | | | | | | |
| $C_0$ ($\mu g\ m^{-3}$) | 2.4 ± 0.1 | 7.6 ± 0.4 | 3.2 ± 0.1 | 2.9 ± 0.3 | 14.1 ± 0.4 | 27 ± 4 | 30 ± 6 | 1.7 ± 0.1 | 89 ± 11 |
| $C_{ss}$ ($\mu g\ m^{-3}$) | 0.5 ± 0.1 | 1.7 ± 0.1 | 2.3 ± 0.1 | 0.3 ± 0.1 | 5.5 ± 0.4 | 18 ± 1 | 21 ± 1 | 3.1 ± 0.2 | 53 ± 3 |
| Experiment #6 (pleated filter, $\rho = 17.6$, UVA) | | | | | | | | | |
| $C_0$ ($\mu g\ m^{-3}$) | 2.1 ± 0.1 | 6.3 ± 0.1 | 2.7 ± 0.6 | 1.9 ± 0.1 | 12.2 ± 0.6 | 29 ± 1 | 33 ± 3 | 2.7 ± 0.3 | 90 ± 6 |
| $C_{ss}$ ($\mu g\ m^{-3}$) | 0.2 ± 0.1 | 0.6 ± 0.1 | 1.2 ± 0.1 | 0.15 ± 0.1 | 2.1 ± 0.1 | 11 ± 1 | 9 ± 1 | 3.2 ± 0.4 | 27 ± 3 |

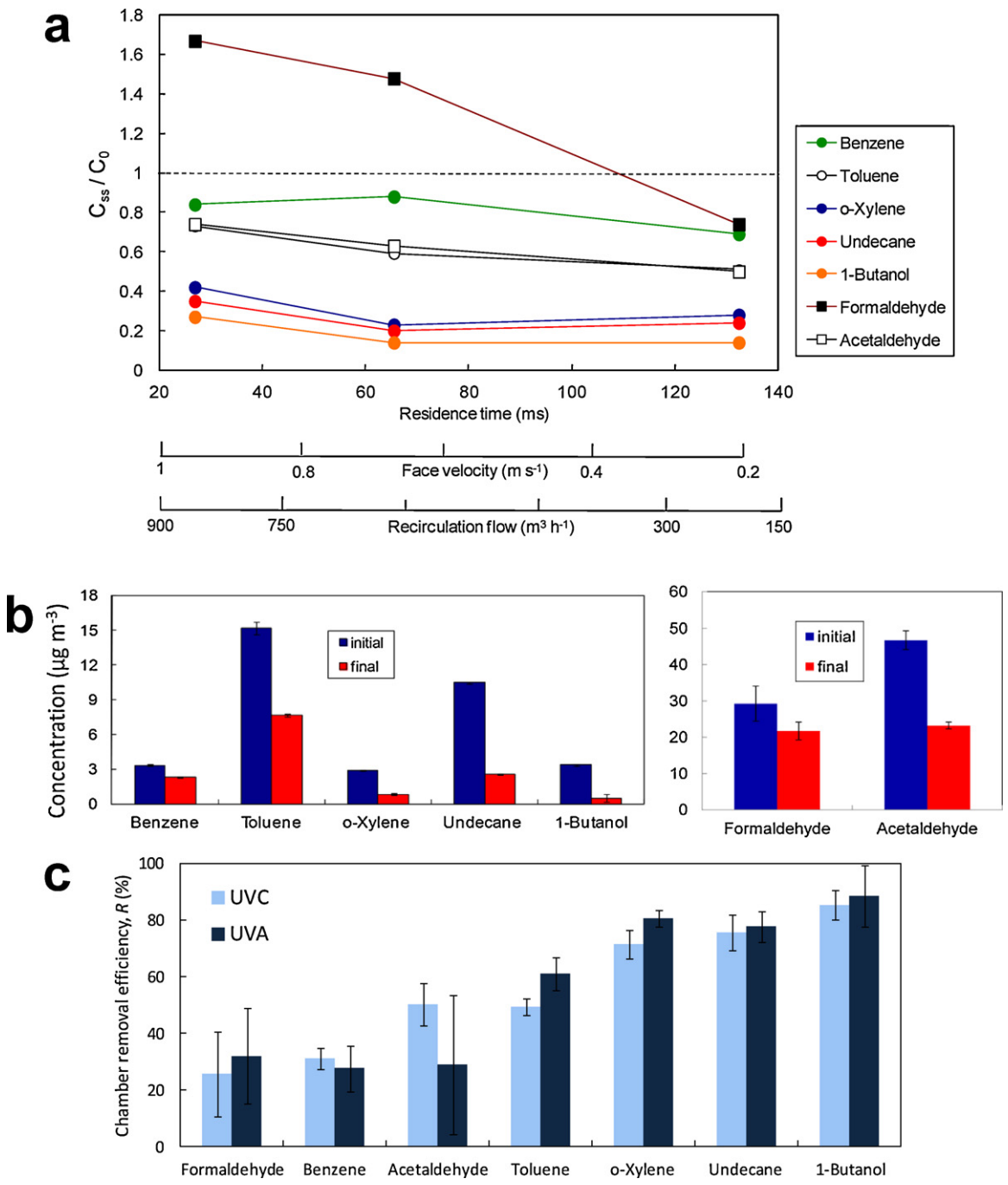


**Fig. 6.** Performance of flat PCO filter. (a) Final-to-initial pollutant concentration ratio ($C_{ss}/C_0$) for experiments carried out at three different recirculation ratios using UVC irradiation; (b) initial and final pollutant concentration at an airflow of 178 $m^3\ h^{-1}$ corresponding to a residence time of 132 ms using UVC irradiation (Experiment #4); (c) removal efficiencies determined using UVC and UVA irradiation at an airflow of 178 and 193 $m^3\ h^{-1}$ respectively, corresponding to residence times of 132 and 122 ms (Experiments #4 and #5).

those that reacted more efficiently at lower residence times, with marginal increases in their removal efficiencies as the recycle ratio decreased. By contrast, the removal efficiency for the more volatile species (formaldehyde, acetaldehyde and benzene) improved significantly as the contact time between the compounds and the PCO media increased. This behavior is consistent with observations reported in the literature in which partitioning between gas phase and the $TiO_2$ hydrated surfaces was shown to be the driver for PCO reactivity [20,30,31]. The improved adsorption of analytes to the media as the airflow decreased is analogous to the well-known effect of the mobile phase flow rate in chromatographic separations predicted by the Van Deemter theory [32]. In addition, it should be considered that the volatile aldehydes are relatively stable byproducts of the photocatalytic oxidation of VOCs. For example, it was recently shown that formaldehyde, acetaldehyde and acetone are the most abundant intermediates in the photooxidation of toluene, remaining in a close loop system over a longer period than the parent compound [21]. For that reason, an extended reaction time window at a lower recirculation rate in our system allowed for a more complete reaction of the byproducts once the precursor VOC had been completely eliminated.

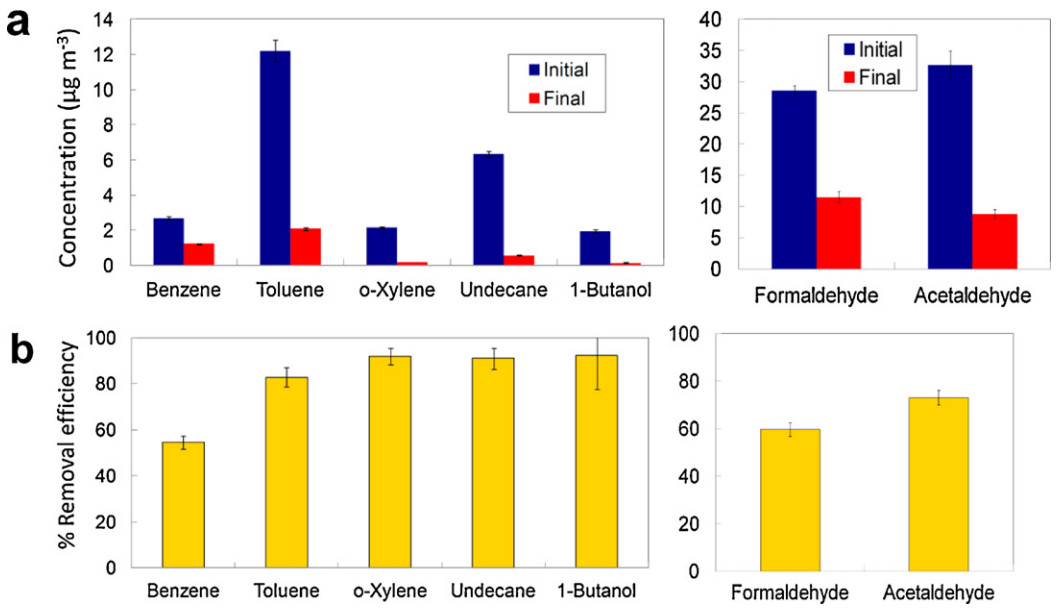


**Fig. 7.** Performance of pleated filter at an airflow of 365 $m^3\ h^{-1}$ corresponding to a residence time of 159 ms (Experiment #6). (a) Initial and final pollutant concentration; (b) removal efficiencies achieved in the same experiment.

The most significant variation in Fig. 6a corresponded to formaldehyde concentrations: the PCO system went from net production of this compound at high recycle ratios to net removal when the airflow was lower than ~300 $m^3\ h^{-1}$ for this particular configuration. This result illustrates the critical role of PCO system design and dimensioning in the effective abatement of this pollutant of concern.

### 3.2. Effect of the type of irradiation

Two of the experiments using the flat PCO filter, #4 and #5, were performed in identical conditions except for the type of irradiation. We used a UVC and a UVA lamp with relatively small differences in irradiance measured at the filter surface (Table 1). Fig. 6b illustrates the concentration changes observed in one of those cases (Experiment #4), and Fig. 6c compares the removal efficiency achieved for each compound in both experiments. Within the experimental error of the determinations, we did not observe a significant change due to the use of UVA lamp over the UVC lamp.

Given the similarities observed in the initial performance of a PCO filter when either a UVC or a UVA lamp is used, future experiments should compare long-term effects associated with the aging of the media, which may be different for each of the lamps depending on their ability to eliminate secondary byproducts formed on the $TiO_2$ surface.

### 3.3. Advantages associated with pleated PCO filters

The dwelling time of compounds on the surface of the irradiated PCO media is one of the most critical parameters that need to be optimized in reactor design. The choice of a flat filter configuration limits the operational airflow rates under optimal PCO performance to values that may not be sufficiently high for certain applications. In the example shown above (Section 3.1), a maximum airflow of 300 $m^3\ h^{-1}$ (face velocity of 0.2 m $s^{-1}$) was required for a net removal of formaldehyde. This limit may be enough for residential applications but not always for commercial HVAC systems. In those cases, the use of pleated filters may make accessible higher contact times between pollutants and the media at higher face velocities. Fig. 7 illustrates the results obtained in Experiment #6 with the pleated filter operating at 365 $m^3\ h^{-1}$.

These results constitute a significant improvement over those achieved with a flat filter. Since the media geometry, the content of $TiO_2$, lamp intensities and irradiation patterns are different for each configuration, it is not possible to carry out a quantitative

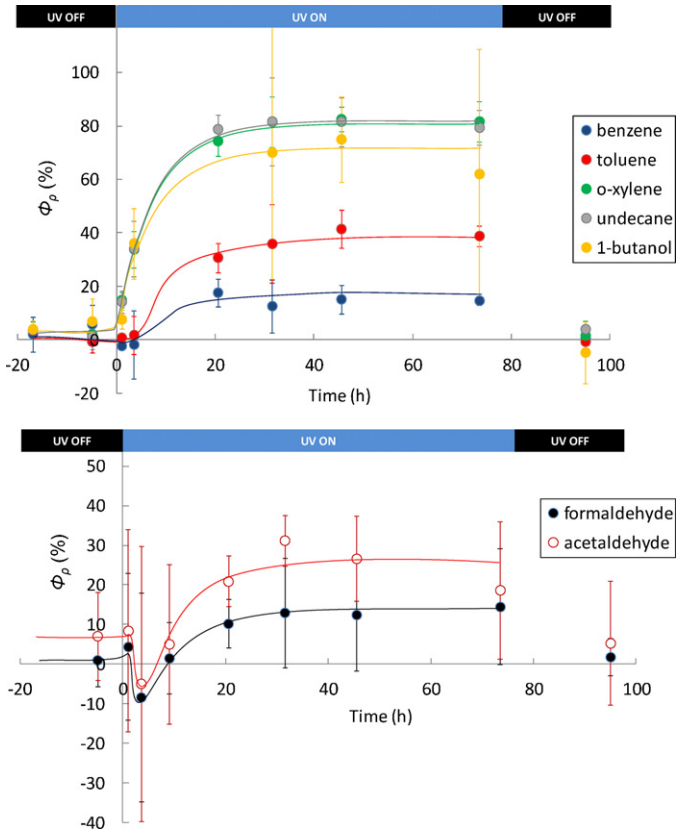


**Fig. 8.** Single-pass removal efficiency $\Phi_\rho$ of analytes as a function of time during experiment using the pleated PCO media (Experiment #6).

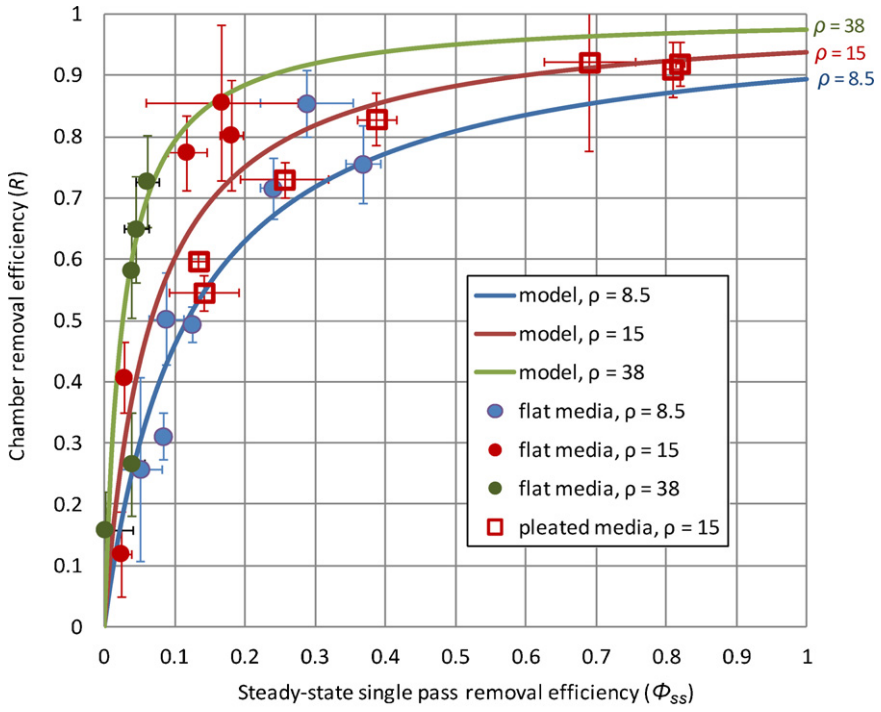


**Fig. 9.** Correlation between global chamber removal efficiency ($R$) and steady-state single-pass removal efficiency ($\Phi_{\rho,ss}$). Solid curves represent solutions to Eq. (5) for the three recycle ratios used in our experiments. Points represent results obtained with flat and pleated media configurations at different recycle ratios.

comparison between experiments carried out with flat and pleated media. However, using the estimated residence time of 159 ms for the pleated filter, the trends observed in Fig. 6a can be extended further and respond to the same qualitative description discussed above. The pleated filter provided enough contact time to achieve very significant net removal efficiency for benzene (>50%) and formaldehyde (59%), and even higher for the remaining pollutants.

### 3.4. Correlation between single-pass removal efficiency and chamber removal efficiency

The changes observed in pollutant chamber concentrations during each test can be described with a simple model that considers a continuous input by the pollutant source, continuous removal by ventilation and a concentration differential introduced by the PCO system operating in an external closed loop, as follows:

$$\frac{\partial c}{\partial t} = k - \lambda c - \rho\lambda(c - c') \quad (1)$$

where $c$ is the chamber concentration of a particular pollutant (in ppb), $k$ is the injection rate of that pollutant (in ppb min$^{-1}$), $\lambda$ is the air exchange rate (in min$^{-1}$), $\rho$ is the recycle ratio (unit-less) and $c'$ is the concentration of the pollutant measured downstream of the PCO media before being mixed with chamber air (in ppb). Before turning on the UV lamp it can be assumed $c = c'$, and at steady state conditions ($\partial c/\partial t = 0$) the parameter $k$ can be calculated as

$$k = \lambda c_0 \quad (2)$$

where $c_0$ is the initial chamber concentration of the pollutant, determined experimentally before turning on the PCO unit.

We also define the single-pass conversion efficiency, $\Phi_\rho(t)$, as:

$$\phi_\rho(t) = 1 - \left(\frac{c'}{c}\right) \quad (3)$$

For each experiment, $\Phi_\rho$ is a function of the irradiation time, as illustrated in Fig. 8 for the test using the pleated media (Experiment #6). In the case of the volatile aldehydes, initial $\Phi_\rho$ values were negative, consistent with net production of these compounds in the early stages as a consequence of partial decomposition of the other VOCs. As the total VOC concentration decreased, the single-pass removal efficiency of the volatile aldehydes increased, switching from negative to positive values (i.e., net removal). Once the

**Table 4**
Steady-state single pass removal efficiency ($\Phi_{\rho,ss}$) and chamber removal efficiency ($R$) determined in experiment with flat and pleated filter media at different recycle ratios ($\rho$).

| | Flat filter $\rho = 38$ (Experiment 3) | | Flat filter $\rho = 15$ (Experiment 2) | | Flat filter $\rho = 8.5$ (Experiment 4) | | Pleated filter $\rho = 15$ (Experiment. 6) | |
|---|---|---|---|---|---|---|---|---|
| | $\Phi_{\rho,ss}$ (%) | $R$ (%) | $\Phi_{\rho,ss}$ (%) | $R$ (%) | $\Phi_{\rho,ss}$ (%) | $R$ (%) | $\Phi_{\rho,ss}$ (%) | $R$ (%) |
| Benzene | n.d. | 16 ± 6 | 2.3 ± 1.5 | 12 ± 7 | 8 ± 1 | 31 ± 4 | 14 ± 5 | 54 ± 3 |
| Toluene | 3.8 ± 1.7 | 26 ± 8 | 2.7 ± 0.8 | 41 ± 6 | 12 ± 1 | 49 ± 3 | 38 ± 3 | 83 ± 4 |
| o-Xylene | 3.7 ± 0.5 | 58 ± 7 | 12 ± 3 | 77 ± 6 | 24 ± 2 | 72 ± 5 | 81 ± 1 | 92 ± 4 |
| Undecane | 4.5 ± 1.8 | 65 ± 9 | 18 ± 2 | 80 ± 9 | 37 ± 3 | 76 ± 6 | 81 ± 2 | 91 ± 5 |
| 1-Butanol | 5.9 ± 1.6 | 73 ± 8 | 16 ± 10 | 85 ± 12 | 29 ± 7 | 85 ± 5 | 69 ± 6 | 92 ± 14 |
| Formaldehyde | n.d. | −66 ± 18 | n.d. | −47 ± 14 | 5 ± 3 | 25 ± 15 | 13 ± 1 | 59 ± 2 |
| Acetaldehyde | n.d. | 25 ± 9 | n.d. | 37 ± 8 | 9 ± 3 | 50 ± 7 | 25 ± 6 | 73 ± 3 |

n.d.: too low $\Phi_{\rho,ss}$ values could not be measured accurately.

system reached steady-state conditions under UV irradiation, the same Eq. (3) can be used to calculate the steady-state single pass removal efficiency ($\Phi_{\rho,ss}$), using the corresponding steady-state concentrations $c_{ss}$ and $c'_{ss}$. Those values were determined experimentally as the average of the final three determinations, for $t > 30$ h. By comparing across the different experiments, we observed that the value of $\Phi_{\rho,ss}$ is also a function of the recycle ratio: it increased as the recycle ratio decreased. This is additional evidence of the effect of increased contact time between the pollutant and the photoactive media at lower recycle ratios.

The chamber removal efficiency $R$ is a global result for the whole experiment, since it compares chamber concentrations measured at steady-state conditions with and without the operation of the PCO air cleaner, all other parameters remaining constant through the test. It is defined as:

$$R = 1 - \left(\frac{c_{ss}}{c_0}\right) \quad (4)$$

Table 4 summarizes the values of $\Phi_{\rho,ss}$ (%) and $R$ (%) determined in experiments with flat and pleated PCO media.

By substituting Eqs. (2)–(4) in Eq. (1), the following expression can be derived to correlate the chamber removal efficiency with the steady-state single pass removal efficiency:

$$R = 1 - \left(\frac{1}{1 + \rho\phi_{\rho,ss}}\right) \quad (5)$$

In the extreme of very low recycle ratios ($\rho \to 0$), the PCO system does not operate efficiently and $R$ tends to zero. In the extreme of very high recycle ratios ($\rho \gg 1$), the chamber removal efficiency can reach optimal levels ($R = 1$) if the single-pass removal efficiency $\Phi_{\rho,ss}$ remains high. However, significant reduction of $\Phi_{\rho,ss}$ can occur due to very low contact times corresponding to the system operating at high recycle ratios. Hence, there is an optimal combination of those two parameters that maximizes the chamber removal efficiency for each compound.

In Fig. 9, we represent Eq. (5) for the three values of recycle ratio used in our experiments: $\rho = 8.5$, 15 and 38. In the same figure we plotted experimental values corresponding to our tests, to verify consistency of our results with the model described by Eq. (5). We confirmed an overall agreement with the model predictions.

## 4. Conclusions

Specific concerns about PCO performance are associated with the formation of volatile aldehydes and other partially oxidized byproducts that can be released back to indoor air. Our results highlight the vital role of design and dimensioning parameters in achieving complete removal of primary pollutants and eliminating or reducing yields of secondary pollutants. Control of these parameters is critical for the safe utilization of PCO systems. In particular, we observed that a sufficiently long contact time between the target compounds and the PCO media is a key factor leading to the complete degradation of primary and secondary pollutants. The dense coated quartz felt used in this experiment is particularly well suited for extending the dwelling time of pollutants in their transit through the air cleaner, by providing a more effective contact with irradiated photocatalyst nanoparticles, as compared with conventional systems in which the $TiO_2$ is deposited on the internal surfaces of a honeycomb monolith. In the flat filter configuration, longer dwelling times were achieved by reducing the face velocity. When design airflow requirements do not allow for sufficient reductions in face velocity, the use of pleated media was shown to increase significantly the system performance. We described a simple correlation between the steady-state single pass removal efficiency and the global chamber removal efficiency, and validated it with the experimental results.

## Acknowledgements

The authors thank W.J. Fisk, M.G. Apte, O. Rosseler, M. Sidheswaran (LBNL) and Prof. P. Pichat (EC Lyon) for helpful suggestions. We also thank R. Maddalena, M. Russell, A. Montalbano (LBNL) and A. Durand (SGQ) for experimental assistance. LBNL is a U.S. Department of Energy laboratory under Contract DE-AC02-05CH11231. The authors also acknowledge Prof. J.-M. Herrmann, to whom this special issue is dedicated. In particular, M. Sleiman expresses his deepest gratitude to Prof. Herrmann, for his support and encouragement throughout his years as a PhD student at LACE/IRCELYON (2004–2008) and until present. Dr. Sleiman feels proud and fortunate to have had the chance to know J.-M.H. the distinguished scientist – whose research for about 40 years contributed significantly to advance our knowledge in the field of catalysis/photocatalysis – but also J.-M.H. the modest, pleasant and generous man that is very enjoyable to be around.

## References

[1] K. Benne, B. Griffith, N. Long, P. Torcellini, Assessment of the energy impacts of outside air in the commercial sector, NREL/TP-550-41955, National Renewable Energy Laboratory, Golden, CO, 2009.
[2] B. Griffith, N. Long, P. Torcellini, R. Judkoff, Methodology for modeling building energy performance across the commercial sector, NREL/TP-550e41956, National Renewable Energy Laboratory, Golden, Co, 2008.
[3] M.A. Sidheswaran, H. Destaillats, D.P. Sullivan, S. Cohn, W.J. Fisk, Building and Environment 47 (2012) 357–367.
[4] M.A. Sidheswaran, H. Destaillats, D.P. Sullivan, J. Larsen, W.J. Fisk, Applied Catalysis B-Environmental 107 (2011) 34–41.
[5] P. Pichat, in: M.A. Tarr (Ed.), Chemical Degradation Methods for Wastes and Pollutants: Environmental and Industrial Applications, Marcel Dekker Inc., New York, Basel, 2003, pp. p77–p119.
[6] M.R. Hoffmann, S.T. Martin, W. Choi, D.W. Bahnemann, Chemical Reviews 95 (1995) 69–96.
[7] P. Pichat, Applied Catalysis B-Environmental 99 (2010) 428–434.
[8] L. Zhong, F. Haghighat, P. Blondeau, J. Kozinski, Building and Environment 45 (2010) 2689–2697.
[9] G.E. Imoberdorf, H.A. Irazoqui, O.M. Alfano, A.E. Cassano, Chemical Engineering Science 62 (2007) 793–804.
[10] C. Passalia, M.E. Martinez Retamar, O.M. Alfano, R.J. Brandi, International Journal of Chemical Reactor Engineering 8 (2010) A161.
[11] D. Vildozo, C. Ferronato, M. Sleiman, J.M. Chovelon, Applied Catalysis B-Environmental 94 (2010) 303–310.
[12] G. Camera-Roda, F. Santarelli, Catalysis Today 129 (2007) 161–168.
[13] G. Li Puma, I. Salvado-Estivill, T.N. Obee, S.O. Hay, Separation and Purification Technology 67 (2009) 226–232.
[14] I. Salvado-Estivill, D.M. Hargreaves, G. Li Puma, Environmental Science & Technology 41 (2007) 2028–2035.
[15] V. Puddu, H. Choi, D.D. Dionysiou, G. Li Puma, Applied Catalysis B-Environmental 94 (2010) 211–218.
[16] M. Grandcolas, A. Louvet, N. Keller, V. Keller, Angewandte Chemie-International Edition 48 (2009) 161–164.
[17] M. Lafjah, F. Djafri, A. Bengueddach, N. Keller, V. Keller, Journal of Hazardous Materials 186 (2011) 1218–1225.
[18] D. Kibanova, M. Trejo, H. Destaillats, J. Cervini-Silva, Applied Clay Science 42 (2009) 563–568.
[19] D. Kibanova, J. Cervini-Silva, H. Destaillats, Environmental Science & Technology 43 (2009) 1500–1506.
[20] A.T. Hodgson, H. Destaillats, D.P. Sullivan, W.J. Fisk, Indoor Air 17 (2007) 305–316.
[21] O. Debono, F. Thevenet, P. Gravejat, V. Hequet, C. Raillard, L. Lecoq, N. Locoge, Applied Catalysis B-Environmental 106 (2011) 600–608.
[22] J. Disdier, P. Pichat, D. Mas, Journal of the Air & Waste Management Association 55 (2005) 88–96.
[23] M. Sleiman, P. Conchon, C. Ferronato, J.M. Chovelon, Applied Catalysis B-Environmental 86 (2009) 159–165.
[24] ANSI/ASHRAE, Method of testing general ventilation air-cleaning devices for removal efficiency by particle size, ANSI/ASHRAE Standard 52.2-2007, Atlanta, GA, ISSN 1041-2336, 2008.
[25] USEPA, Method TO-1, Revision 1,0: Method for the determination of volatile organic compounds in ambient air using Tenax® Adsorption and gas chromatography/mass spectrometry (GC/MS), Center for Environmental Research Information, Office of Research and Development US Environmental Protection Agency, 1984.
[26] USEPA, Compendium Method TO-11A – Determination of formaldehyde in ambient air using adsorbent cartridge followed by HPLC [active sampling methodology], Office of Research and Development – US Environmental Protection Agency, Cincinnati, OH, 1999.

[27] A. Maudhuit, C. Raillard, V. Hequet, L. Le Coq, J. Sablayrolles, L. Molins, Chemical Engineering Journal 170 (2011) 464–470.
[28] N. Quici, M.L. Vera, H. Choi, G. Li Puma, D.D. Dionysiou, M.I. Litter, H. Destaillats, Applied Catalysis B-Environmental 95 (2010) 312–319.
[29] O. Debono, PhD Thesis, Ecole de Mines de Nantes, France, 2011.
[30] C. Raillard, V. Hequet, P. Le Cloirec, J. Legrand, Journal of Photochemistry and Photobiology A: Chemistry 163 (2004) 425–431.
[31] M.E. Zorn, S.O. Hay, M.A. Anderson, Applied Catalysis B-Environmental 99 (2010) 420–427.
[32] D.A. Skoog, F.J. Holler, S.R. Crouch, Principles of Instrumental Analysis, 6th edition, Thomson, Brooks/Cole, Belmont, CA, 2007.
[33] A.T. Hodgson, H. Levin., Classification of measured indoor volatile organic compounds based on noncancer health and comfort considerations. LBNL report # 53308 (2003). http://www.inive.org/members_area/medias/pdf/Inive/LBL/LBNL-53308.pdf.
[34] D. Shimer, T.J. Phillips, P.L. Jenkins, 2005. Report to the California Legislature. Indoor Air Pollution in California (2005). http://www.arb.ca.gov/research/indoor/ab1173/rpt0705.pdf.
[35] F.J. Offermann., Ventilation and Indoor Air Quality in New Homes. California Air Resources Board and California Energy Commission, PIER Energy Related Environmental Research Program. Collaborative Report. CEC 500 2009 085 (2009). http://www.arb.ca.gov/research/apr/past/04-310.pdf.